Initiation and evolution of an isolated submarine canyon system on a low-gradient continental slope

Wei Li [a, b] *, Shuang Li [a, b], Tiago M. Alves [c], Song Jing[a], Hongjun Chen[d] *, Wenhuan Zhan [a, b]

[a] CAS Key Laboratory of Ocean and Marginal Sea Geology, South China Sea Institute of Oceanology, Chinese Academy of Sciences, Guangzhou 510301, China

[b] University of Chinese Academy of Sciences, Beijing 100049, China

[c] 3D Seismic Lab, School of Earth and Environmental Sciences, Cardiff University, Main Building, Park Place, Cardiff, CF10 3AT, United Kingdom

[d] MLR Laboratory of Marine Mineral Resources, Guangzhou Marine Geological Survey, Guangzhou 510250, China

Correspondence to: Dr. Wei Li (wli@scsio.ac.cn) and Dr. Hongjun Chen (chjchj578578@gmail.com)

Abstract

Submarine canyons are important conduits transferring large volumes of sediment, nutrients, and pollutants from the continental shelf to deep-water basins. However, the mechanisms initiating submarine canyons and the factors influencing their evolution are still poorly understood. Here, we use multibeam bathymetry and two-dimensional seismic reflection data to investigate the origin and development of a submarine canyon system on the northern South China Sea margin. Our results show a submarine canyon system lying at a water depth of 400-1200 m on a relatively low-gradient (<0.5°), open continental slope. At the bottom of this canyon system, buried canyons undercut a mass-transport complex (MTC 1), whose top surface is early Pliocene in age. No other modern or buried canyons, channels and gullies are observed outside the area spanned by MTC 1. Such an observation demonstrates that pre-existing slide

scars can capture gravity flows by providing accommodation space for sediment transported onto the lower continental slope, thus facilitating the development of pre-existing channels above MTCs. Lateral accretion packages identified on the southwest walls of several submarine canyons suggest they migrated northeastward due to the influence of contour currents. In addition, the presence of several basal erosional surfaces and smaller-scale MTCs in the canyons confirms they have undergone multiple cut-and-fill cycles, which were likely controlled by relative sea-level changes. The relative high sea level recorded at present ultimately led to the preservation of the studied canyon system on the continental slope. The results not only demonstrate the crucial role of submarine landslides in the initiation of submarine canyons, but also highlight how relative changes in sea level influence the evolution of submarine canyons on low-gradient continental slopes.

Keywords: Submarine landslides; mass-transport complexes; submarine canyons; canyon initiation; South China Sea.

1 Introduction

Submarine canyons, as key elements in deep-water depositional systems, are common morphological features on continental margins (Shepard, 1972; Puig et al., 2014; Sweet and Blum, 2016; Fisher et al., 2021). By incising continental shelves and slopes, they act as major pathways for sediment, nutrients and pollutants transported into deep-marine environments (Santora et al., 2018; Kane et al., 2020; Pierdomenico et al., 2020; Serra et al., 2020; Bernhardt

and Schwanghart, 2021; Zhong and Peng, 2021). Submarine canyons can also record high levels of biodiversity, impact the spatial distribution of marine habitats, comprising at the same time a valuable resource for education and research (Santora et al., 2018; Pierdomenico et al., 2019). Below the seafloor, submarine canyons are able to influence the trapping and release of gas hydrates by changing local geothermal conditions and sedimentary architecture (Davies et al., 2012; Benjamin et al., 2015; Crutchley et al., 2017).

The initiation of submarine canyons and their subsequent development is controlled by factors such as sediment supply (Puig et al., 2017; Jipa and Panin et al., 2020; Li et al., 2021), tectonics (Le Dantec et al., 2010; Micallef et al., 2014; Naranjo-Vesga et al., 2022), sea-level change (Rasmussen et al., 1994; Zecchin et al., 2011; Allin et al., 2018), slope topography (Li et al., 2020), oceanographic currents (e.g. Shanmugam, 2003; Puig et al., 2004), and so on. Turbidity currents and mass-wasting events are considered to be the most common processes shaping submarine canyons (Harris and Whiteway, 2011). Based on the position of canyon heads on the shelf break, two main types of submarine canyon system have previously been recognised: a) shelf-incising, and b) slope-confined canyons (Jobe et al., 2011). Shelf-incising canyons are known to indent continental shelves and can be linked to major river systems. Turbidity currents entraining coarse-grained shelf sediment are considered to play a critical role in their development (Smith et al., 2018; Nanson et al., 2022). Conversely, slope-confined canyons with apexes situated below the shelf break are completely disconnected from onshore drainage systems (Jobe et al., 2011; Huang et al., 2014; Post et al., 2022). Their onset is related to slope failure, with mass wasting retrogressively eroding the continental slope and retreating landwards to form new canyon heads (Jobe et al., 2011; Mulder et al., 2012; Tubau et al., 2013).

Strikingly, submarine canyon systems consisting of shelf-incising and slope-confined canyons are always linked, to a certain degree, to point-sources of sediment via the development of prodeltas (e.g., Great Barrier Reef margin and Shenhu Canyon system), or because they develop on narrow continental shelves where sediment bypass predominates, as in the case of the western and central Mediterranean and the USA's Atlantic margin (Puga-Bernabé et al., 2013; Brothers et al., 2013; Li et al., 2015; Chiocci and Casalbore, 2017; Ercilla et al., 2022).

Submarine canyons and MTCs have been widely documented in the Pearl River Mouth Basin of the northern South China Sea (e.g. Ding et al., 2013; He et al., 2014; Zhao et al., 2015; Sun et al., 2018; Hui et al., 2019; Tian et al., 2021). Previous studies have mostly focused on the morphology, internal architecture and evolution of submarine canyons of the Shenhu Canyon System (e.g. Zhu et al., 2010; Qiao et al., 2015; Yin et al., 2019; Su et al., 2020). The onset of these submarine canyons was considered to be related to the presence of bottom-current sediment waves (Wang et al., 2023). Their evolution was proposed to be influenced by the interaction of turbidity currents and contour currents, resulting in their unidirectional migration with time (e.g. Zhu et al., 2010; Gong et al., 2013; Zhou et al., 2015; Gong et al., 2018). In comparison, the Pearl River Canyon is the largest submarine canyon in the Pearl River Mouth Basin, acting as the major pathway for sediment transported from the continental shelf to the abyssal plain (e.g. Ding et al., 2013; Wang et al., 2014). Its initiation was influenced by the combined effect of eustasy, sediment supply and Cenozoic tectonics (Ding et al., 2013). In addition, multiple slope failures have occurred in the PRMB, resulting in the formation of numerous MTCs (e.g. Li et al., 2014; Wang et al., 2017; Sun et al., 2018). Previous work have focused on the formation mechanism and evolution of submarine canyons and MTCs separately,

but it is still unclear whether the initiation of submarine canyons relates to the occurrence of MTCs in the northern South China Sea.

In this study, a submarine canyon system in the South China Sea is investigated using multibeam bathymetry data and two-dimensional seismic reflection profiles (Fig. 1). Located at a water depth of 400 m to 1200 m, the canyon system of interest comprises a total of six submarine canyons (Chen et al., 2017). In contrast to other systems addressed in the literature, the canyon system is located ~270 km to the south of the present-day shoreline (Fig. 1), putting in question if the factors controlling its initiation and evolution are similar to other canyon systems in the South China Sea. Therefore, a comprehensive analysis of this canyon system is presented in this work with the ultimate aim of: (a) investigating canyon morphology in great detail; (b) analysing the internal depositional architecture of discrete canyons; (c) discussing the causes that lead to the initiation of canyons; and (d) determining the factors affecting canyon evolution.

2 Geological and oceanographic settings

2.1 Geological setting

The South China Sea, as one of the largest marginal seas in the world with an area of c. 3.5×10^6 km^2, is located at the junction of the Eurasian, Pacific and Australia-India plates (Taylor and Hayes, 1980). Here, continental rifting started at ~65 Ma and subsequent continental breakup propagated from northeast to southwest (Briais et al., 1993; Barckhausen et al., 2014). Diachronous seafloor spreading occurred from 33 Ma to 15 Ma in the northeast, and 23.6 Ma to 16 Ma in the southwest of the South China Sea (Li et al., 2015; Zhao et al.,

2016).

In the northern part of the South China Sea margin occur multiple Cenozoic basins; the Yinggehai and Qiongdongnan basins in the southwest, the Pearl River Mouth Basin in its central part, and the Taixinan Basin in the northeast (Xie et al., 2006). The Pearl River Mouth Basin (PRMB) is the largest sedimentary basin of the four, with an area of ~175,000 km^2 (Fig. 1a). Three main tectonic episodes are revealed in seismic, borehole and biostratigraphic data: (1) the first episode (Paleocene to the Early Oligocene) recorded multiple pulses of continental rifting and fluvial-lacustrine sediments accumulated in relatively isolated basins (Zhu et al., 2010); (2) from Late Oligocene to Early Miocene, a syn-breakup episode witnessed the abrupt subsidence of rift basins and deposition of coastal-littoral sediments (Xie et al., 2014; Zhao et al., 2016); (3) in the third episode, post-rift subsidence and a gradual rise in sea level led to the accumulation of marine deposits in the PRMB since the Middle Miocene (Gong et al., 1989; Wu et al. 2005) (Fig. 2). Importantly, from 23.8 Ma to 21.0 Ma, the shelf break migrated northwards to its present location, from a position ~100 km south of the modern shelf break. At present, the continental shelf has a depth of 20 m to 220 m, an average width of ~240 km, and a gradient of 0.05-0.06° (Huang et al., 1996).

2.2 Oceanographic setting

Water masses in the South China Sea comprise a seasonally influenced surface water and permanent intermediate and deep waters (Chen et al., 2014; Gan et al., 2016). Surface water occurs up to a depth of 350 m, and its flow is governed by the East Asia monsoon system (Lüdmann et al., 2005). Due to bi-annual monsoon changes, surface water masses flow

counterclockwise during winter, but clockwise in the summer (Zhu et al., 2010). The clockwise-flowing intermediate water masses - commonly named the 'Kuroshio Current' - were established in the Late Miocene and span a water depth from 350 m to 1500 m (Xie et al., 2013; Wang et al., 2014) (Fig. 1a). In contrast, counterclockwise deep-water flows are promoted by the incursion of the south-flowing North Pacific Deep Water into the South China Sea via the Luzon Strait (Lüdmann et al., 2005) (Fig. 1a). The average velocity of deep-water masses exceeds 0.15 m/s, with a maximum velocity up to 0.3 m/s at water depths around 2500 to 2600 m (Xie et al., 2009).

3 Data and methods

The bathymetric data used in this work were acquired by Guangzhou Marine Geological Survey at a water depth ranging from 400 m to 1200 m and positioned by a differential GPS. The data were processed with a horizontal resolution of ~100 m, and a vertical resolution between ~1 m and 3.3 m, using the software CARIS HIPS®. The bathymetric data were interpreted in ArcMap 10.8.1 and Global Mapper® V22. Canyon morphology, including mean width, incision depth and slope gradient, are extracted using Spatial Analysis and Hydrology tools in ArcMap 10.8.1.

Regional 2D seismic data were acquired by the China National Offshore Oil Corporation using a 3000-m long streamer with 240 channels. The acquisition geometry produced seismic traces with a spacing of 12.5 m. The seismic signal was generated using a 3850 cubic-inch air gun, with a vertical resolution of 15-20 m. The acquired seismic data is zero-phased and

displayed with a Society of Exploration Geophysicists' normal polarity, suggesting red reflection on the seismic profiles represents the positive reflection event (Brown, 2011). The frequency bandwidth of the seismic data is 30-45 Hz and their interpretation was carried out on Geoframe® 4.5.

Two regional stratigraphic horizons, named T1 (5.5 Ma) and T2 (10.5 Ma), are identified in the study area. The first horizon (T1) represents an important post-rift stratigraphic boundary generated after the end of seafloor spreading in the South China Sea. It marks the boundary between Upper Miocene and Pliocene strata. The older horizon (T2) separates Middle and Upper Miocene strata.

4 Results

4.1 Modern canyon morphology

The submarine canyon system of interest consists of six canyons (C1 to C6) occurring at a water depth from 400 m to 1200 m (Figs. 1b and 3a). Bathymetric maps show the seafloor around the submarine canyons as having a relatively gentle gradient of ~0.3°. The length of the canyons ranges from 7.2 km (C5) to 25 km (C2) (Fig. 4a and Table 1). Their width increases gradually downslope in canyons C2, C3 and C6, but remains constant in C1, C4 and C5 (Table 1; Figs. 3 and 4b). The average incision depth of the submarine canyons varies from 53 m (C5) to 164 m (C3) (Table 1; Fig. 4b). Canyons C1 and C6 have a maximum slope gradient of ~1.5° along their thalwegs (Table 1). Canyons C2 and C3 have asymmetric walls in their upper and lower reaches, and their northeast walls are much steeper than their southwest counterparts

(Figs. 5b and c). However, wall gradients are similar in the lower reaches of C2 and C3 (Fig. 5c). The canyon heads of C2 and C3 gradually migrate northeastward towards the upper continental slope, while C1, C4 to C6 are relatively straight (Figs. 3a and 5a). A tributary abuts the west side of canyon C3, which starts at a water depth of ~600 m and merges into the main thalweg at 700 m (Fig. 3a).

At a water depth of 1200 m, other canyon systems are identified towards the lower continental slope such as the Yitong Canyon in the southeast and several unnamed canyons to the southwest (Fig. 1b). A large field of sediment waves is observed covering both canyons and interfluves in the lower part of this canyon system (Figs. 3a and b).

4.2 Internal seismic architecture of submarine-canyon fills

Zoomed-in seismic sections crossing canyons C2, C3 and C4 provide information on their internal architectures (Figs. 6-9). The canyons' basal erosional surfaces are V- and U-shaped along continuous seismic reflections with a positive polarity and high- to medium amplitudes (Figs. 8a, c and e). The base of the three canyons cuts into, or is located immediately above, the top surface of MTC 1 (Figs. 6 and 7). Stacking patterns of seismic reflections in the canyons reveal lateral migration to the northeast (Figs. 8b, d and f). In parallel, canyon fills show two different types of seismic facies, as described below.

The first type of seismic facies is characterised by a series of stacked, continuous inclined seismic reflectors that are generally parallel or sub-parallel to each other on the flanks of southwest canyons (Figs. 6 and 7). Together with these vertically stacked canyon walls, a series of lateral accretion packages (LAPs), 1- 4 km wide 120-300 m thick (0.6 s-1.0 s), can be

196 identified (Figs. 8a, c and e).

197 Other seismic facies filling the canyons comprise chaotic and low- to medium-amplitude
198 seismic reflectors with low continuity (Figs. 8a, c and e). There are no other modern or buried
199 erosional features (e.g., smaller canyons, channels or gullies) around the canyons of interest to
200 this work, as Pliocene to Quaternary strata show continuous and parallel seismic reflections
201 (Figs. 10a, b and c). Although a deeply buried V-shaped canyon is identified to the northeast
202 of the canyon system (corresponding to the location of C1), no other depressions are observed
203 between C1 and C6 (Fig. 10).

204

205 **4.3 Buried mass-transport complexes**

206 Two buried MTCs are imaged below the canyon system of interest in Figs. 6, 7, 9 and 10.
207 Based on the established regional seismic stratigraphy, MTC 1 and MTC 2 occur in Pliocene
208 and Upper Miocene strata, respectively. The shallower and younger MTC 1 (Figs. 6 and 7), the
209 focus of this study, underlies canyons C1 to C6 (Figs. 6 and 7).

210 Interpreted on NE-SW seismic profiles, the basal shear zone of MTC 1 is generally parallel
211 or sub-parallel to the seismic reflections below (Figs. 6 and 7). Zoomed-in seismic sections
212 reveal remarkable basal ramps and blocks in MTC 1 (Figs. 6b and 7b). Its top surface is also
213 rugged and several V- and U-shaped depressions are imaged in Figs. 6 and 7. Seismic profiles
214 show that MTC 1 is almost entirely evacuated along its lateral scarp to the west (Figs. 6 and 7).

5 Discussion

5.1 Initiation of submarine canyons over buried MTCs

The initiation of submarine canyons has been attributed to multiple causes (Harris and Whiteway, 2011; Hui et al., 2019). Oversteepening of the continental slope caused by sea-level change, faulting and tectonic uplift, can trigger long-term slope-grading processes (erosional mass wasting and depositional processes) to generate new submarine canyons (Ross et al., 1994). Though several faults can be identified in the study area, the slope gradient of the palaeo-seafloor is quite similar to the modern seabed (Fig. 9). This suggests that oversteepening may not be the main mechanism explaining the generation of submarine canyons in the study area. Dense water cascading (DWC) developing as near-bottom gravity currents play a significant role in forming and shaping submarine canyons (Canal et al., 2006; Allen et al., 2009; Puig et al., 2014). Mauffrey et al. (2017) also emphasised the role of sea-level changes and fluvial connection on submarine-canyon initiation. However, the submarine canyon system in this work has been far away (i.e. isolated) from the South China coast since the latest Miocene (5.5 Ma), excluding the DWC as responsible for its onset. A recent study has proposed that the troughs between bottom-current sediment waves can capture sediment gravity flows, resulting in the initiation of submarine canyons (Wang et al., 2023). Due to the absence of bottom-current sediment waves (their crests should be parallel with the canyons), we do not consider this mechanism as a plausible in the study area.

The canyon system interpreted in this work is different from the slope-confined submarine canyon systems previously documented in the PRMB by Zhou et al. (2015), Li et al. (2016)

and Yin et al. (2019). It also differs from canyon systems offshore the Little Bahama Bank (Mulder et al., 2012; Tournadour et al., 2017), SE Brazil (Qin et al., 2017) and northeast Australian margin (Puga-Bernabéu et al., 2013). In the study area, the average seafloor gradient of the modern continental slope is low (<0.5°) when compared to the slope-confined canyon systems of the Bahamas and northeast Australia (2°-10°). The absence of canyon heads on the shelf edge - at a water depth from 380-650 m to 200-300 m and 30 to 55 km distant from the shelf break - excludes shelf-incising processes as responsible for the development of canyons C1 to C6. The lower reaches of submarine canyons are also not directly connected to the basin floor or abyssal plain; they rather disappear gradually downslope at a water depth of 800-1400 m (Figs. 1b and 3a). Except for buried canyons to the northeast of canyon C2 and C6 (Figs. 7c and 10d), no other submarine canyons, channels or even erosional gullies are identified near the studied canyon system (Fig. 1b). This suggests that the canyons of interest are confined and isolated, giving rise to three important questions on their origin and evolution: (1) how and when were these submarine canyons initiated? (2) how did they evolve since their formation? (3) which controlling factors influenced their evolution?

The rugged top surface of MTC 1 shows multiple V- and U-shaped depressions; the occurrence of frequent gravity flows and subsequent incision of MTC 1 after its emplacement may be responsible for the formation of these depressions as no linear undercut features are observed along its basal glide zone (Figs. 6 and 7). The overlapping and undercutting of canyons C2, C3 and C4 on MTC 1 demonstrates that V- and U-shaped depressions constitute an early form of submarine canyons (Figs. 6b and 7b). Although the seismic profiles show that MTC 2 has occurred before the early Tortonian (10.5 Ma), the sea-level curve indicates a

relative highstand after its formation (Fig. 2). This suggests that the relative location of MTC 2 was too far away from sediment sources on the continental shelf to trigger frequent gravity flows. Moreover, contour currents can act as an important sediment redistributor on the seafloor (Bernhardt et al., 2015). The strata above MTC 2 show continuous and sub-parallel seismic reflections, indicating that sediment deposition in this area was dominantly governed by contour currents. The long distance from the sediment sources, combined with the influence of contour currents, resulted in the absence of submarine canyons after the emplacement of MTC 2.

Chen et al. (2017) first documented the presence of the submarine canyon system of interest to this study. They proposed a close relationship between submarine canyons and the underlying submarine landslide. However, it is still unclear why these submarine canyons only developed in the study area with no other canyons, channels or gullies identified in their vicinity. Recent data from the western Somali Basin off Tanzania indicates that large-scale submarine landslides were a primary control on the evolution of sediment transfer zones along continental margins (Stagna et al., 2023). Evacuation zones associated with submarine landslides generate 'conveyor belts' where increasing seafloor gradients can trap land-derived materials, focusing sediment point sources. Similar examples are documented in the Baiyun Slide Complex (Li et al., 2020, in SE Brazil (Qin et al., 2017), and on the SE Australian continental margin (Wu et al., 2022), areas where submarine landslides produced an erosional morphology capable of capture gravity flows that further erode the seafloor. Several submarine channels in the headwall area of the Baiyun Slide Complex were formed after its last phase of instability (Li et al., 2020). The initiation of channels was associated with the evacuation of the Baiyun Slide

scar, where a large volume of seafloor sediment was removed and subsequent turbidity currents and mass-wasting flows could be accommodated within the landslide scar. Along SE Brazil and the southeast Australian continental margins, slide scars generated by retrogressive slope failure were able to capture gravity flows sourced from the continental shelf and upper continental slope, thus developing areas of flow convergence that helped widening and deepening the canyons (Qin et al., 2017; Wu et al., 2022). Thus, this paper supports the hypothesis that an evacuated landslide scar accommodated gravity flows from the upper continental slope, promoting the development of canyons C1-C6.

The present-day sea level is relatively high when compared to when the submarine canyons were first incised in the study area, and so is the distance between the canyons and the shoreline. The shelf break thus appears to have retreated significantly on a low-gradient continental margin after 5.5. Ma, making the submarine canyons appear isolated on the broad, open continental slope of the northern South China Sea.

5.2 Factors controlling the evolution of submarine canyons

High-resolution seismic profiles reveal lateral accretion packages (LAPs) in C2, C3 and C4 that are typical of a northeast migration of canyons during their development (Fig. 8). Canyon migration is mainly controlled by external factors such as the Coriolis force and/or interactions between turbidity and contour currents. The Coriolis force can change the direction of gravity flows to the right in the Northern Hemisphere and to the left in the Southern Hemisphere. Thus, more erosion would be expected on the western walls of submarine canyons in the South China Sea, while enhanced deposition should occur on their eastern walls. Yet, the

Coriolis force can be excluded as a main factor controlling canyon migration in the study area due to the greater incision depths of their northeast sides (Figs. 5b and 5c). Similar unidirectionally migrating canyons have been documented in other regions of the northern South China Sea margin such as the Shenhu Canyon System and northeast Qiongdongnan margin, where the development of LAPs on their western walls are considered a result of interacting turbidity and contour currents (He et al., 2013; Gong et al., 2013; Zhou et al., 2015; Su et al., 2020). In addition, Rodrigues et al. (2020) proposed that submarine canyons developing within a mixed (turbidite-contourite) system, with strong and persistent bottom currents, migrate with the contour current direction. Our study area is affected by Intermediate Water circulation since the middle Miocene (Zhu et al., 2010; Chen et al., 2014), which may be responsible for the long-term northeastward migration of canyons C1 to C6.

Seismic sections reveal the presence of multiple basal erosional surfaces interbedded with LAPs (Fig. 8). Such a character suggests the importance of multiple cut-and-fill episodes during the development of the LAPs. Rasmussen (1994) investigated the seismic facies during cut-and-fill cycles on the continental slope of the coast of south Gabon. Sediment deposition caused by lateral accretion within the South Gabon canyons was considered to only occur during relative sea-level lowstands. The northern South China Sea has undergone multiple cycles of relative sea-level rise and fall since the Pliocene (Fig. 2). Sediment is more easily delivered to deep-water basins through erosional canyons during sea-level lowstands as the shelf break is closer to the canyon heads. In such lowstand periods, LAPs and erosion were coeval under the combined influence of contour and turbidity currents. During sea-level highstands, hemipelagic deposition predominated in the canyons, enabling the filling

characterised by a horizontal, sub-parallel facies within the submarine canyons of our interest (Fig. 8). Therefore, we suggest that the development of isolated canyon systems on the low-gradient, open continental slope of northern South China Sea was controlled by relative sea level and the effect of contour currents.

Here, we propose a schematic model comprising four main stages to summarise how the isolated canyon system in our study area has evolved since the early Pliocene (Fig. 11).

(a) Stage I: A submarine landslide was triggered in the early Pliocene, formed a broad slide scar, followed by the deposition of MTC 1 within this same scar.

(b) Stage II: After the emplacement of MTC 1, gravity flows were captured by its scar and led to the formation of erosive channels on the top surface of MTC 1.

(c) Under the continuous erosion of gravity flows, some of the pre-existing channels were widened and deepened, generating early-stage submarine canyons. Together with northeast-flowing contour currents, relative sea-level change resulted in multiple cut-and-fill cycles within the canyons and contributed to the unidirectional migration of LAPs.

(d) Later, some of the canyons were made inactive and buried, while canyons C2 to C4 are still active at present. The modern sea level is higher than the period after the initiation of submarine canyons and this caused the shelf break to retreat for tens of kilometers on a low-gradient (<0.5°) continental slope. Isolated submarine canyon systems were thus preserved on an open continental slope.

6 Conclusions

This work investigates a submarine canyon system on the northern South China Sea margin in terms of its origin and development processes using multibeam bathymetric data and 2D seismic profiles. Its main conclusions are as follows.

(1) The submarine canyons in this study are isolated on a low-gradient, open continental slope with no other modern submarine canyons, channels or even erosional gullies in their vicinity.

(2) A submarine landslide (MTC 1) occurred before the onset of the submarine canyons. The resulting slide scar captured and confined the gravity flows sourced from the upper continental slope, leading to the first incision of submarine canyons.

(3) The canyons underwent multiple cut-and-fill cycles due to changes in relative sea level since the early Pliocene.

(4) Northeast-flowing bottom currents interacting with downslope turbidity currents are responsible for the unidirectional migration of the submarine canyons in this study.

Our analysis offers new insights into the origin and evolution of an isolated submarine canyon system on low-gradient continental slopes. We use this case-study to illustrate the significant role of slope instability in the initiation of submarine canyons, providing information applicable to other landslide-prone continental margins.

Acknowledgments

We are grateful to China National Offshore Oil Corporation for their permission to release

the seismic data used in this work. Guangdong Basic and Applied Basic Research Foundation (2020B1515020016), National Scientific Foundation of China (41876054), Hainan Provincial Joint Project of Sanya Yazhou Bay Science and Technology City (420LHO48) are acknowledged for providing the funding. Dr. Wei Li is specially funded by CAS Pioneer Hundred Talents Program (Y8SL011001). We are grateful to the editors (Prof. Zhongyuan Chen and Prof. Ziyin Wu), as well as Dianele Casalbore and one anonymous reviewer for their constructive comments that greatly improved the quality of this manuscript.

References

Allen, S., Durrieu de Madron, X., 2009. A review of the role of submarine canyons in deep-ocean exchange with the shelf. Ocean Science, 5(4), 607-620.

Allin, J.R., Hunt, J.E., Clare, M.A., Talling, P.J., 2018. Eustatic sea-level controls on the flushing of a shelf-incising submarine canyon. GSA Bulletin, 130(1-2), 222-237.

Barckhausen, U., Engels, M., Franke, D., Ladage, S., Pubellier, M., 2014. Evolution of the South China Sea: Revised ages for breakup and seafloor spreading. Marine and Petroleum Geology, 58, 599-611.

Benjamin, U., Huuse, M., Hodgetts, D., 2015. Canyon-confined pockmarks on the western Niger Delta slope. Journal of African Earth Sciences, 107, 15-27.

Bernhardt, A., Melnick, D., Jara-Muñoz, J., Argandoña, B., González, J., Strecker, M. R., 2015. Controls on submarine canyon activity during sea-level highstands: The Biobío canyon system offshore Chile. Geosphere, 11(4), 1226-1255.

Bernhardt, A., Schwanghart, W., 2021. Where and why do submarine canyons remain connected to the shore during sea-level rise? Insights from global topographic analysis and Bayesian regression. Geophysical

Research Letters, 48(10), e2020GL092234.

Briais, A., Patriat, P., Tapponnier, P., 1993. Updated interpretation of magnetic anomalies and seafloor spreading stages in the South China Sea: Implications for the Tertiary tectonics of Southeast Asia. Journal of Geophysical Research: Solid Earth, 98(B4), 6299-6328.

Brothers, D.S., Uri, S., Andrews, B.D., Chaytor, J.D., Twichell, D.C., 2013. Geomorphic process fingerprints in submarine canyons. Marine Geology 337, 53-66.

Brown, A. R., 2011. Interpretation of three-dimensional seismic data. Society of Exploration Geophysicists and American Association of Petroleum Geologists.

Canals, M., Puig, P., de Madron, X.D., Heussner, S., Palanques, A., Fabres, J., 2006. Flushing submarine canyons. Nature, 444(7117), 354-357.

Chen, H., Xie, X., Van Rooij, D., Vandorpe, T., Su, M., Wang, D., 2014. Depositional characteristics and processes of alongslope currents related to a seamount on the northwestern margin of the Northwest Sub-Basin, South China Sea. Marine Geology, 355, 36-53.

Chiocci, F. L., & Casalbore, D. 2017. Unexpected fast rate of morphological evolution of geologically-active continental margins during Quaternary: Examples from selected areas in the Italian seas. Marine and Petroleum Geology, 82, 154-162.

Chen, H., Zhan, W., Li, L., Wen, M.-m., 2017. Occurrence of submarine canyons, sediment waves and mass movements along the northern continental slope of the South China Sea. Journal of Earth System Science, 126, 1-28.

Crutchley, G., Kroeger, K., Pecher, I., Mountjoy, J., Gorman, A., 2017. Gas hydrate formation amid submarine canyon incision: investigations from New Zealand's Hikurangi subduction margin. Geochemistry, Geophysics, Geosystems, 18(12), 4299-4316.

Davies, R.J., Thatcher, K.E., Mathias, S.A., Yang, J., 2012. Deepwater canyons: An escape route for methane sealed by methane hydrate. Earth and Planetary Science Letters, 323, 72-78.

Ding, W., Li, J., Li, J., Fang, Y., Tang, Y., 2013. Morphotectonics and evolutionary controls on the Pearl River canyon system, South China Sea. Marine Geophysical Research, 34, 221-238.

Ercilla, G., Galindo-Zaldívar, J., Estrada, F., Valencia, J., Juan, C., Casas, D., Alonso, B., Comas, M.C., Tendero-Salmerón, V., Casalbore, D., 2022. Understanding the complex geomorphology of a deep sea area affected by continental tectonic indentation: The case of the Gulf of Vera (Western Mediterranean). Geomorphology 402, 108126.

Fisher, W.L., Galloway, W.E., Steel, R.J., Olariu, C., Kerans, C., Mohrig, D., 2021. Deep-water depositional systems supplied by shelf-incising submarine canyons: Recognition and significance in the geologic record. Earth-Science Reviews, 214, 103531.

Gan, J., Liu, Z., Hui, C.R., 2016. A three-layer alternating spinning circulation in the South China Sea. Journal of Physical Oceanography, 46(8), 2309-2315.

Gong, Z., Jin, Q., Qiu, Z., Wang, S., Meng, J., 1989. Geology, tectonics and evolution of the Pearl River Mouth Basin. Chinese Sedimentary Basins. Elsevier, Amsterdam, 181, 196.

Gong, C., Wang, Y., Zhu, W., Li, W., Xu, Q., 2013. Upper Miocene to Quaternary unidirectionally migrating deep-water channels in the Pearl River Mouth Basin, northern South China SeaUnidirectionally Migrating Deep-Water Channels. AAPG bulletin, 97(2), 285-308.

Gong, C., Wang, Y., Rebesco, M., Salon, S., Steel, R.J., 2018. How do turbidity flows interact with contour currents in unidirectionally migrating deep-water channels? Geology, 46(6), 551-554.

Haq, B.U., Hardenbol, J., Vail, P.R., 1987. Chronology of fluctuating sea levels since the Triassic. Science, 235(4793), 1156-1167.

Harris, P.T., Whiteway, T., 2011. Global distribution of large submarine canyons: Geomorphic differences between active and passive continental margins. Marine Geology, 285(1-4), 69-86.

He, Y., Xie, X., Kneller, B.C., Wang, Z., Li, X., 2013. Architecture and controlling factors of canyon fills on the shelf margin in the Qiongdongnan Basin, northern South China Sea. Marine and Petroleum Geology, 41, 264-276.

He, Y., Zhong, G., Wang, L., Kuang, Z., 2014. Characteristics and occurrence of submarine canyon-associated landslides in the middle of the northern continental slope, South China Sea. Marine and Petroleum Geology, 57, 546-560.

Huang, Z., Zhang, W., Chai, F., 1996. The submerged Zhujiang Delta (in Chinese). Oceanographic Literature Review, 3(43), 251.

Huang, Z., Nichol, S.L., Harris, P.T., Caley, M.J., 2014. Classification of submarine canyons of the Australian continental margin. Marine Geology, 357, 362-383.

Hui, G., Li, S., Guo, L., Somerville, I.D., Wang, P., Wang, Q., 2019. Mechanisms of submarine canyon formation on the northern continental slope of the South China Sea. Geological Journal, 54(6), 3389-3403.

Jipa, D.C., Panin, N., 2020. Narrow shelf canyons vs. wide shelf canyons: Two distinct types of Black Sea submarine canyons. Quaternary International, 540, 120-136.

Jobe, Z.R., Lowe, D.R., Uchytil, S.J., 2011. Two fundamentally different types of submarine canyons along the continental margin of Equatorial Guinea. Marine and Petroleum Geology, 28(3), 843-860.

Kane, I.A., Clare, M.A., Miramontes, E., Wogelius, R., Rothwell, J.J., Garreau, P., Pohl, F., 2020. Seafloor microplastic hotspots controlled by deep-sea circulation. Science, 368(6495), 1140-1145.

Le Dantec, N., Hogarth, L.J., Driscoll, N.W., Babcock, J.M., Barnhardt, W.A., Schwab, W.C., 2010. Tectonic

452 controls on nearshore sediment accumulation and submarine canyon morphology offshore La Jolla,
453 Southern California. Marine Geology, 268(1-4), 115-128.
454 Li, W., Wu, S., Völker, D., Zhao, F., Mi, L., Kopf, A., 2014. Morphology, seismic characterization and
455 sediment dynamics of the Baiyun Slide Complex on the northern South China Sea margin. Journal of
456 the Geological Society, 171(6), 865-877.
457 Li, C.F., Li, J., Ding, W., Franke, D., Yao, Y., Shi, H., Pang, X., Cao, Y., Lin, J., Kulhanek, D.K., 2015.
458 Seismic stratigraphy of the central South China Sea basin and implications for neotectonics. Journal of
459 Geophysical Research: Solid Earth, 120(3), 1377-1399.
460 Li, W., Alves, T.M., Rebesco, M., Sun, J., Li, J., Li, S., Wu, S., 2020. The Baiyun Slide Complex, South
461 China Sea: A modern example of slope instability controlling submarine-channel incision on
462 continental slopes. Marine and Petroleum Geology, 114, 104231.
463 Li, W., Li, S., Alves, T.M., Rebesco, M., Feng, Y., 2021. The role of sediment gravity flows on the
464 morphological development of a large submarine canyon (Taiwan Canyon), north-east South China Sea.
465 Sedimentology, 68(3), 1091-1108.
466 Mauffrey, M.-A., Urgeles, R., Berné, S., Canning, J., 2017. Development of submarine canyons after the
467 Mid-Pleistocene Transition on the Ebro margin, NW Mediterranean: The role of fluvial connections.
468 Quaternary Science Reviews, 158, 77-93.
469 Micallef, A., Mountjoy, J.J., Barnes, P.M., Canals, M., Lastras, G., 2014. Geomorphic response of submarine
470 canyons to tectonic activity: Insights from the Cook Strait canyon system, New Zealand. Geosphere,
471 10(5), 905-929.
472 Miramontes, E., Eggenhuisen, J.T., Jacinto, R.S., Poneti, G., Pohl, F., Normandeau, A., Campbell, D.C.,
473 Hernández-Molina, F.J., 2020. Channel-levee evolution in combined contour current–turbidity current

474 flows from flume-tank experiments. Geology, 48(4), 353-357.
475 Moscardelli, L., Wood, L., 2008. New classification system for mass transport complexes in offshore
476 Trinidad. Basin research, 20(1), 73-98.
477 Mulder, T., Ducassou, E., Gillet, H., Hanquiez, V., Tournadour, E., Combes, J., Eberli, G.P., Kindler, P.,
478 Gonthier, E., Conesa, G., Robin, C., Sianipar, R., Reijmer, J.J.G., François, A., 2012. Canyon
479 morphology on a modern carbonate slope of the Bahamas: Evidence of regional tectonic tilting.
480 Geology, 40(9), 771-774.
481 Nanson, R.A., Borissova, I., Huang, Z., Post, A., Nichol, S.L., Spinoccia, M., Siwabessy, J.W., Sikes, E.L.,
482 Picard, K., 2022. Cretaceous to Cenozoic controls on the genesis of the shelf-incising Perth Canyon;
483 insights from a two-part geomorphology mapping approach. Marine Geology, 445, 106731.
484 Naranjo-Vesga, J., Paniagua-Arroyave, J., Ortiz-Karpf, A., Jobe, Z., Wood, L., Galindo, P., Shumaker, L.,
485 Mateus-Tarazona, D., 2022. Controls on submarine canyon morphology along a convergent tectonic
486 margin. The Southern Caribbean of Colombia. Marine and Petroleum Geology, 137, 105493.
487 Paull, C., Ussler III, W., Holbrook, W., 2007. Assessing methane release from the colossal Storegga
488 submarine landslide. Geophysical research letters, 34(4).
489 Pierdomenico, M., Casalbore, D., & Chiocci, F. L. (2020). The key role of canyons in funnelling litter to the
490 deep sea: A study of the Gioia Canyon (Southern Tyrrhenian Sea). Anthropocene, 30, 100237.
491 Pierdomenico, M., Cardone, F., Carluccio, A., Casalbore, D., Chiocci, F., Maiorano, P., & D'Onghia, G.
492 (2019). Megafauna distribution along active submarine canyons of the central Mediterranean:
493 Relationships with environmental variables. Progress in Oceanography, 171, 49-69.
494 Post, A.L., Przeslawski, R., Nanson, R., Siwabessy, J., Smith, D., Kirkendale, L.A., Wilson, N.G., 2022.
495 Modern dynamics, morphology and habitats of slope-confined canyons on the northwest Australian

496 margin. Marine Geology, 443, 106694.
497 Puig, P., Palanques, A., Martín, J., 2014. Contemporary sediment-transport processes in submarine canyons.
498 Annual review of marine science, 6, 53-77.
499 Puga-Bernabéu, Á., Webster, J.M., Beaman, R.J., Guilbaud, V., 2013. Variation in canyon morphology on
500 the Great Barrier Reef margin, north-eastern Australia: The influence of slope and barrier reefs.
501 Geomorphology, 191, 35-50.
502 Puig, P., Palanques, A., Guillén, J., 2004. Role of internal waves in the generation of nepheloid layers on the
503 northwestern Alboran slope: Implications for continental margin shaping. Journal of Geophysical
504 Research: Oceans, 109(C9).
505 Puig, P., Durán, R., Muñoz, A., Elvira, E., Guillén, J., 2017. Submarine canyon-head morphologies and
506 inferred sediment transport processes in the Alías-Almanzora canyon system (SW Mediterranean): On
507 the role of the sediment supply. Marine Geology, 393, 21-34.
508 Qin, Y., Alves, T.M., Constantine, J., 2017. The role of mass wasting in the progressive development of
509 submarine channels (Espirito Santo Basin, SE Brazil). Journal of Sedimentary Research, 87(5): 500-
510 516.
511 Qiao, S., Su, M., Kuang, Z., Yang, R., Liang, J., Wu, N., 2015. Canyon-related undulation structures in the
512 Shenhu area, northern South China Sea. Marine Geophysical Research, 36, 243-252.
513 Rasmussen, E.S., 1994. The relationship between submarine canyon fill and sea-level change: an example
514 from Middle Miocene offshore Gabon, West Africa. Sedimentary Geology, 90(1-2), 61-75.
515 Rodrigues, S., Hernández-Molina, F. J., Fonnesu, M., Miramontes, E., Rebesco, M., Campbell, D. C., 2022.
516 A new classification system for mixed (turbidite-contourite) depositional systems: Examples,
517 conceptual models and diagnostic criteria for modern and ancient records. Earth-Science Reviews, 230,

104030.

Ross, W., Halliwell, B., May, J., Watts, D., Syvitski, J., 1994. Slope readjustment: a new model for the development of submarine fans and aprons. Geology, 22(6), 511-514.

Santora, J.A., Zeno, R., Dorman, J.G., Sydeman, W.J., 2018. Submarine canyons represent an essential habitat network for krill hotspots in a Large Marine Ecosystem. Scientific Reports, 8(1), 1-9.

Serra, C.S., Martínez-Loriente, S., Gràcia, E., Urgeles, R., Vizcaino, A., Perea, H., Bartolome, R., Pallàs, R., Iacono, C.L., Diez, S., 2020. Tectonic evolution, geomorphology and influence of bottom currents along a large submarine canyon system: The São Vicente Canyon (SW Iberian margin). Marine Geology, 426, 106219.

Shanmugam, G., 2003. Deep-marine tidal bottom currents and their reworked sands in modern and ancient submarine canyons. Marine and Petroleum Geology, 20(5): 471-491.

Shepard, F.P., 1972. Submarine canyons. Earth-Science Reviews, 8(1), 1-12.

Smith, M.E., Werner, S.H., Buscombe, D., Finnegan, N.J., Sumner, E.J., Mueller, E.R., 2018. Seeking the shore: Evidence for active submarine canyon head incision due to coarse sediment supply and focusing of wave energy. Geophysical Research Letters, 45(22), 12,403-412,413.

Su, M., Lin, Z., Wang, C., Kuang, Z., Liang, J., Chen, H., Liu, S., Zhang, B., Luo, K., Huang, S., 2020. Geomorphologic and infilling characteristics of the slope-confined submarine canyons in the Pearl River Mouth Basin, northern South China Sea. Marine Geology, 424, 106166.

Sun, Q., Cartwright, J., Xie, X., Lu, X., Yuan, S., Chen, C., 2018. Reconstruction of repeated Quaternary slope failures in the northern South China Sea. Marine Geology, 401, 17-35.

Stagna, M.D., Maselli, V., van Vliet, A., 2023. Large-scale submarine landslide drives long-lasting regime shift in slope sediment deposition. Geology.

Sweet, M.L., Blum, M.D., 2016. Connections Between Fluvial To Shallow Marine Environments and Submarine Canyons: Implications For Sediment Transfer To Deep Water. Journal of Sedimentary Research, 86(10), 1147-1162.

Taylor, B., Hayes, D.E., 1980. The tectonic evolution of the South China Basin. Washington DC American Geophysical Union Geophysical Monograph Series, 23, 89-104.

Tian, H., Lin, C., Zhang, Z., Li, H., Zhang, B., Zhang, M., Liu, H., Jiang, J., 2021. Depositional architecture, evolution and controlling factors of the Miocene submarine canyon system in the Pearl River Mouth Basin, northern South China Sea. Marine and Petroleum Geology, 128, 104990.

Tournadour, E., Mulder, T., Borgomano, J., Gillet, H., Chabaud, L., Ducassou, E., Hanquiez, V., Etienne, S., 2017. Submarine canyon morphologies and evolution in modern carbonate settings: The northern slope of Little Bahama Bank, Bahamas. Marine Geology, 391, 76-97.

Tubau, X., Lastras, G., Canals, M., Micallef, A., Amblas, D., 2013. Significance of the fine drainage pattern for submarine canyon evolution: The Foix Canyon System, Northwestern Mediterranean Sea. Geomorphology, 184, 20-37.

Wang, L., Wu, S.-G., Li, Q.-P., Wang, D.-W., Fu, S.-Y., 2014. Architecture and development of a multi-stage Baiyun submarine slide complex in the Pearl River Canyon, northern South China Sea. Geo-Marine Letters, 34, 327-343.

Wang, X., Wang, Y., He, M., Chen, W., Zhuo, H., Gao, S., Wang, M., Zhou, J., 2017. Genesis and evolution of the mass transport deposits in the middle segment of the Pearl River canyon, South China Sea: Insights from 3D seismic data. Marine and Petroleum Geology, 88, 555-574.

Wang, X., Kneller, B., Sun, Q., 2023. Sediment waves control origins of submarine canyons. Geology, 51(3), 310-314.

562 Wu, S., Yu, Z., Zhang, R., Han, W., Zou, D., 2005. Mesozoic–Cenozoic tectonic evolution of the Zhuanghai
563 area, Bohai-Bay Basin, east China: the application of balanced cross-sections. Journal of Geophysics
564 and Engineering 2, 158-168.
565 Wu, N., Nugraha, H.D., Zhong, G., Steventon, M.J., 2022. The role of mass-transport complexes in the
566 initiation and evolution of submarine canyons. Sedimentology, 69(5), 2181-2202.
567 Xie, X., Müller, R.D., Li, S., 2006. Origin of anomalous subsidence along the Northern South China Sea
568 margin and its relationship to dynamic topography. Marine and Petroleum Geology, 23(7): 745-765.
569 Xie, L., Tian, J., Hu, D., Wang, F., 2009. A quasi-synoptic interpretation of water mass distribution and
570 circulation in the western North Pacific II: Circulation. Chinese Journal of Oceanology and Limnology,
571 27(4), 955-965.
572 Xie, Q., Xiao, J., Wang, D., Yu, Y., 2013. Analysis of deep-layer and bottom circulations in the South China
573 Sea based on eight quasi-global ocean model outputs. Chinese Science Bulletin, 58(32), 4000-4011.
574 Xie, H., Zhou, D., Li, Y., 2014. Cenozoic tectonic subsidence in deepwater sags in the Pearl River Mouth
575 Basin, northern South China Sea. Tectonophysics, 615: 182-198.
576 Yin, S., Lin, L., Pope, E.L., Li, J., Ding, W., Wu, Z., Ding, W., Gao, J., Zhao, D., 2019. Continental slope-
577 confined canyons in the Pearl River Mouth Basin in the South China Sea dominated by erosion, 2004–
578 2018. Geomorphology, 344, 60-74.
579 Zecchin, M., Caffau, M., Roda, C., 2011. Relationships between high-magnitude relative sea-level changes
580 and filling of a coarse-grained submarine canyon (Pleistocene, Ionian Calabria, Southern Italy).
581 Sedimentology, 58(4), 1030-1064.
582 Zhao, F., Alves, T.M., Li, W., Wu, S., 2015. Recurrent slope failure enhancing source rock burial depth and
583 seal unit competence in the Pearl River Mouth Basin, offshore South China Sea. Tectonophysics, 643,

584 1-7.
585 Zhao, F., Alves, T.M., Wu, S., Li, W., Huuse, M., Mi, L., Sun, Q., Ma, B., 2016. Prolonged post-rift
586 magmatism on highly extended crust of divergent continental margins (Baiyun Sag, South China Sea).
587 Earth and Planetary Science Letters, 445, 79-91.
588 Zhong, G., Peng, X., 2021. Transport and accumulation of plastic litter in submarine canyons—The role of
589 gravity flows. Geology, 49(5), 581-586.
590 Zhou, W., Wang, Y.M., Gao, X.Z., Zhu, W.L., Xu, Q., Xu, S., Cao, J.Z., Wu, J., 2015. Architecture, evolution
591 history and controlling factors of the Baiyun submarine canyon system from the middle Miocene to
592 Quaternary in the Pearl River Mouth Basin, northern South China Sea. Marine and Petroleum Geology,
593 67, 389-407.
594 Zhu, M., Graham, S., Pang, X., McHargue, T., 2010. Characteristics of migrating submarine canyons from
595 the middle Miocene to present: Implications for paleoceanographic circulation, northern South China
596 Sea. Marine and Petroleum Geology, 27(1), 307-319.
597

Figures

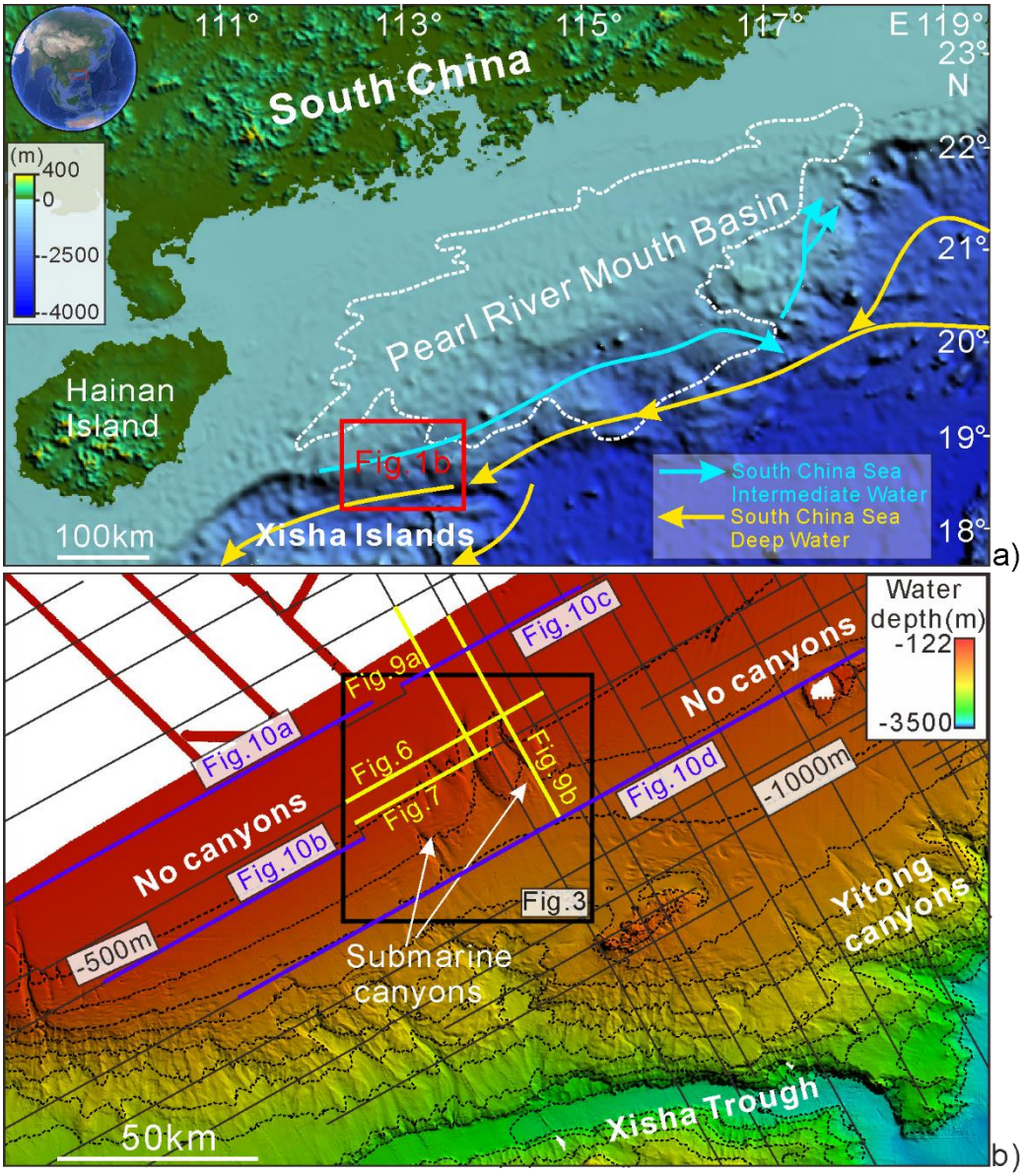

Figure 1 (a) General bathymetric map highlighting the location of the study area. The white dotted line marks the boundary of the Pearl River Mouth Basin. (b) Bathymetric map plotted with 250 m contour lines revealing the isolated submarine canyon system of interest to this work. The black solid lines mark the location of the 2D seismic profiles acquired in the study area. Blue and yellow solid lines represent the location of seismic profiles in Figs. 6, 7, 9 and 10.

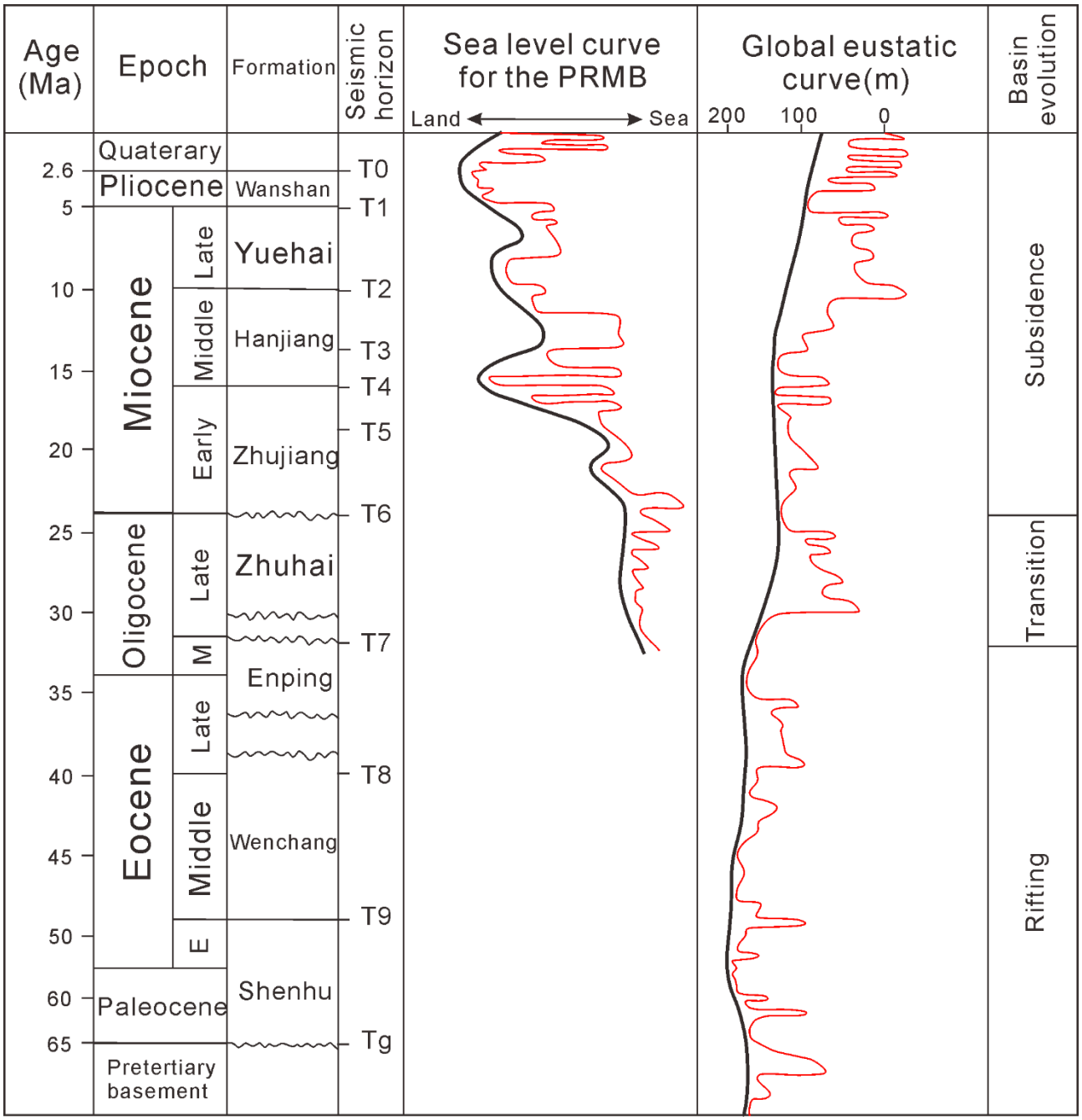

Figure 2 Main stratigraphic units of the Pearl River Mouth Basin and corresponding basin evolution. The sea-level curves plotted in the figure indicate the global and PRMB eustatic variations following Haq et al. (1987), Xie et al. (2014) and Chen et al. (2018). Black and red solid curves respectively show 2nd and 3rd-order sea-level changes.

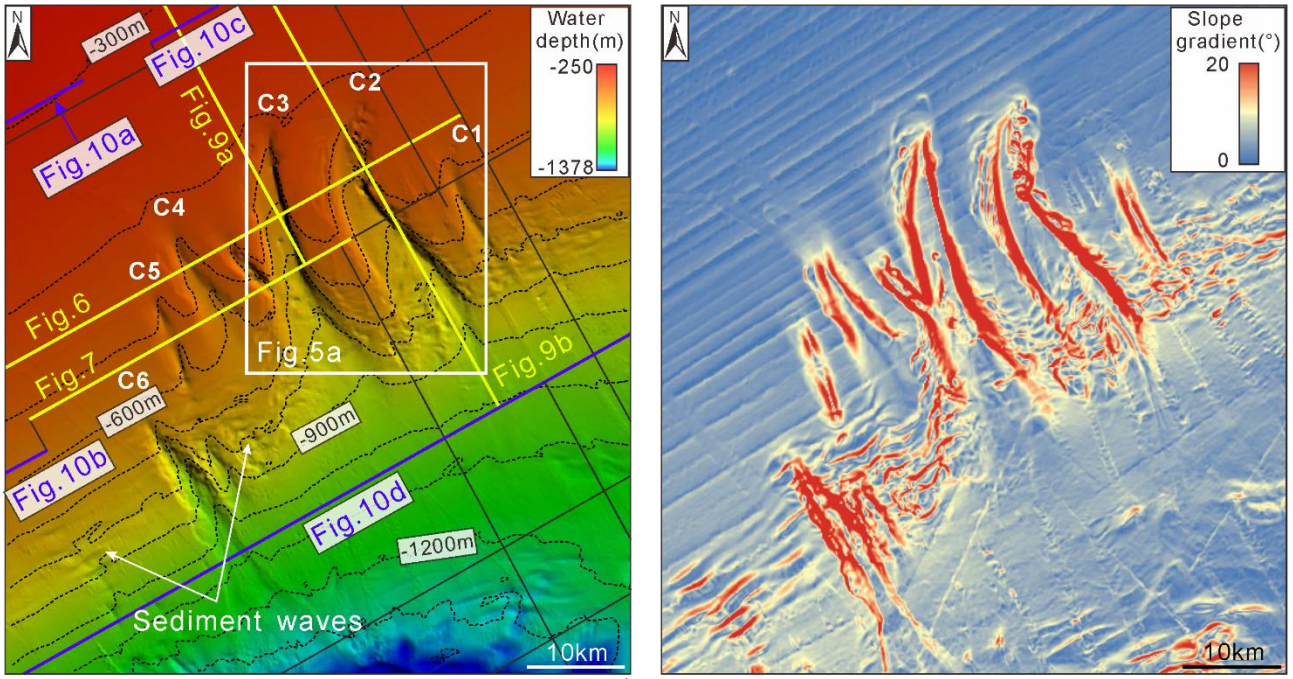

Figure 3 (a) Zoomed-in bathymetric map with 100 m contours showing submarine canyons C1 to C6 on the continental slope of the northern South China Sea. A field of sediment waves is identified in the lower reaches of these six submarine canyons. Black solid lines show the distribution of seismic lines in this area. (b) Slope gradient map of the isolated submarine canyon system and surrounding area.

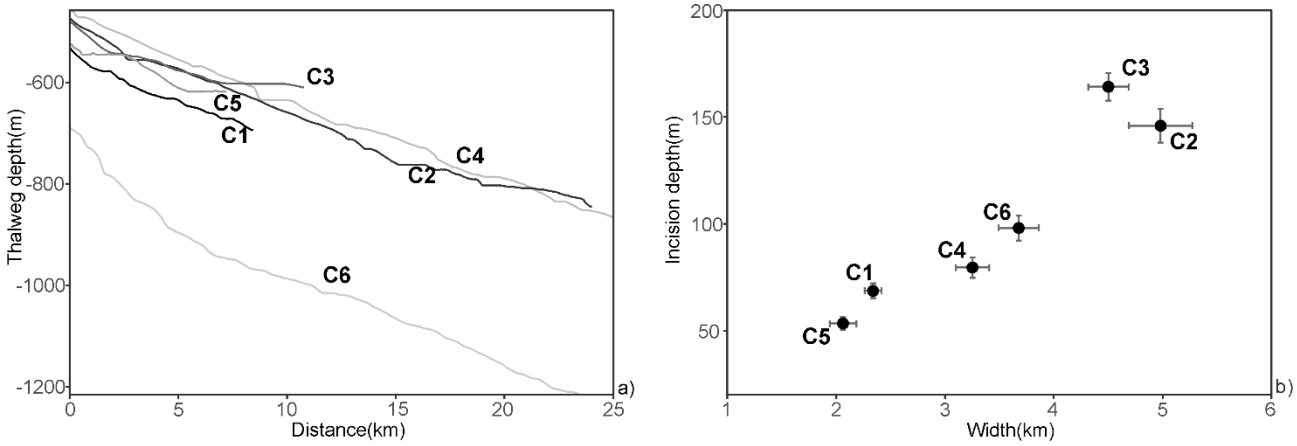

Figure 4 (a) Thalweg depth for canyons C1 to C6 from their head to their mouths as extracted from Arcmap 10.8.1. (b) Scatter plots showing the canyons' mean width against mean incision depth. Standard deviation in the measured values is also shown.

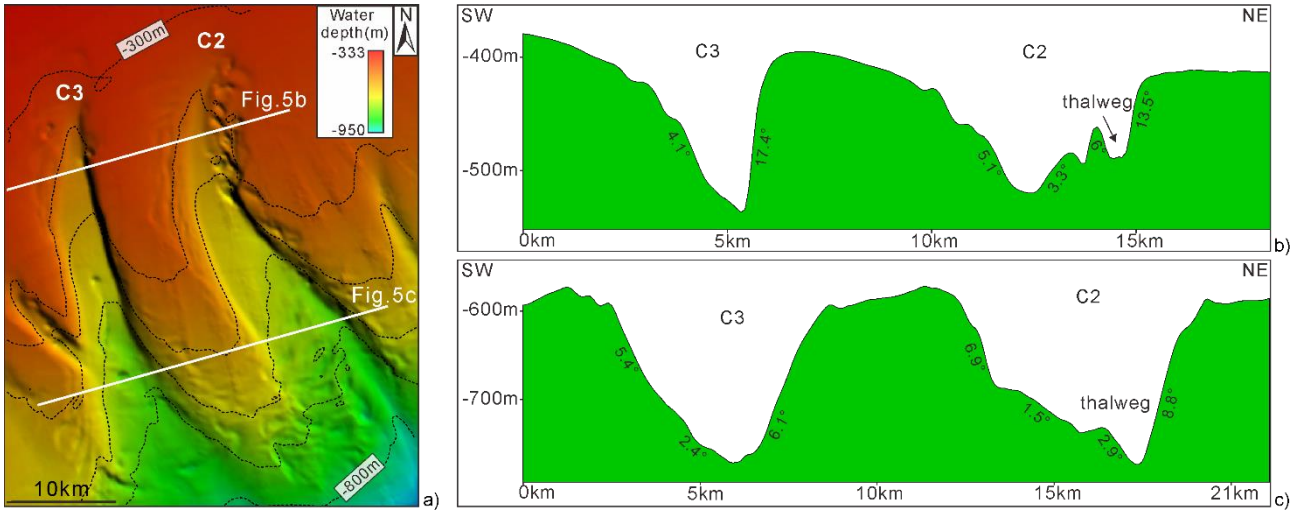

621

622 Figure 5 (a) Zoomed-in bathymetric map with 100 m contour lines highlighting the lateral
623 migration of C2 and C3 towards the northeast near the canyon heads. (b) and (c) SW-NE cross-
624 sections respectively showing the upper and lower reaches of both canyons. Slope gradients
625 are gentler on the southwest walls when compared to the northeast walls of canyons C2 and
626 C3.

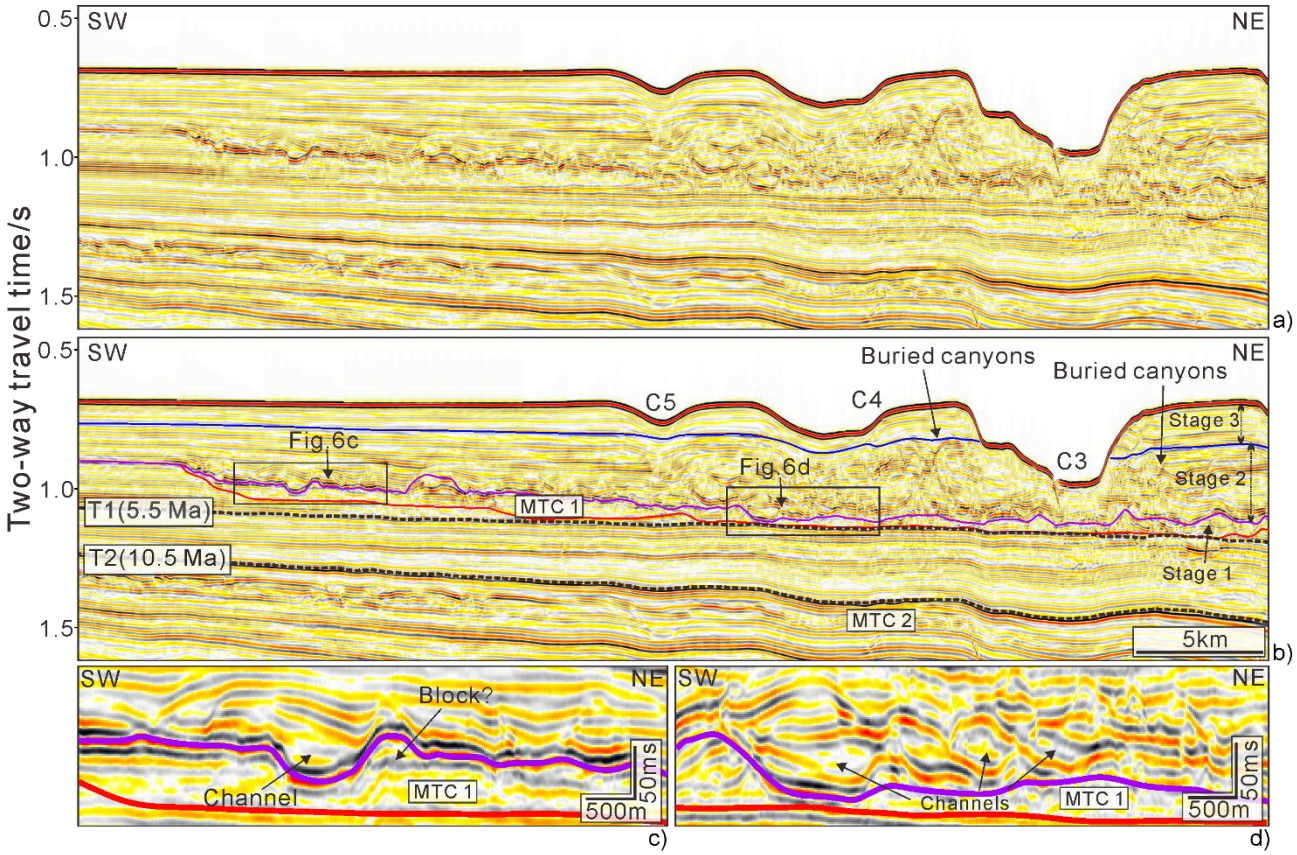

627

Figure 6 (a) Uninterpreted seismic profiles across canyons C3, C4 and C5. (b) Seismic profiles highlighting two regional seismic-stratigraphic markers (5.5 Ma and 10.5 Ma) and the internal architecture in and around the submarine canyons. Purple and red solid lines mark the top and base of MTC 1. The three evolution stages described in this work are marked on the profile, with the blue line revealing the boundary between Stages 2 and 3. (c) and (d) Zoomed-in seismic profiles showing erosive channels on top of MTC 1.

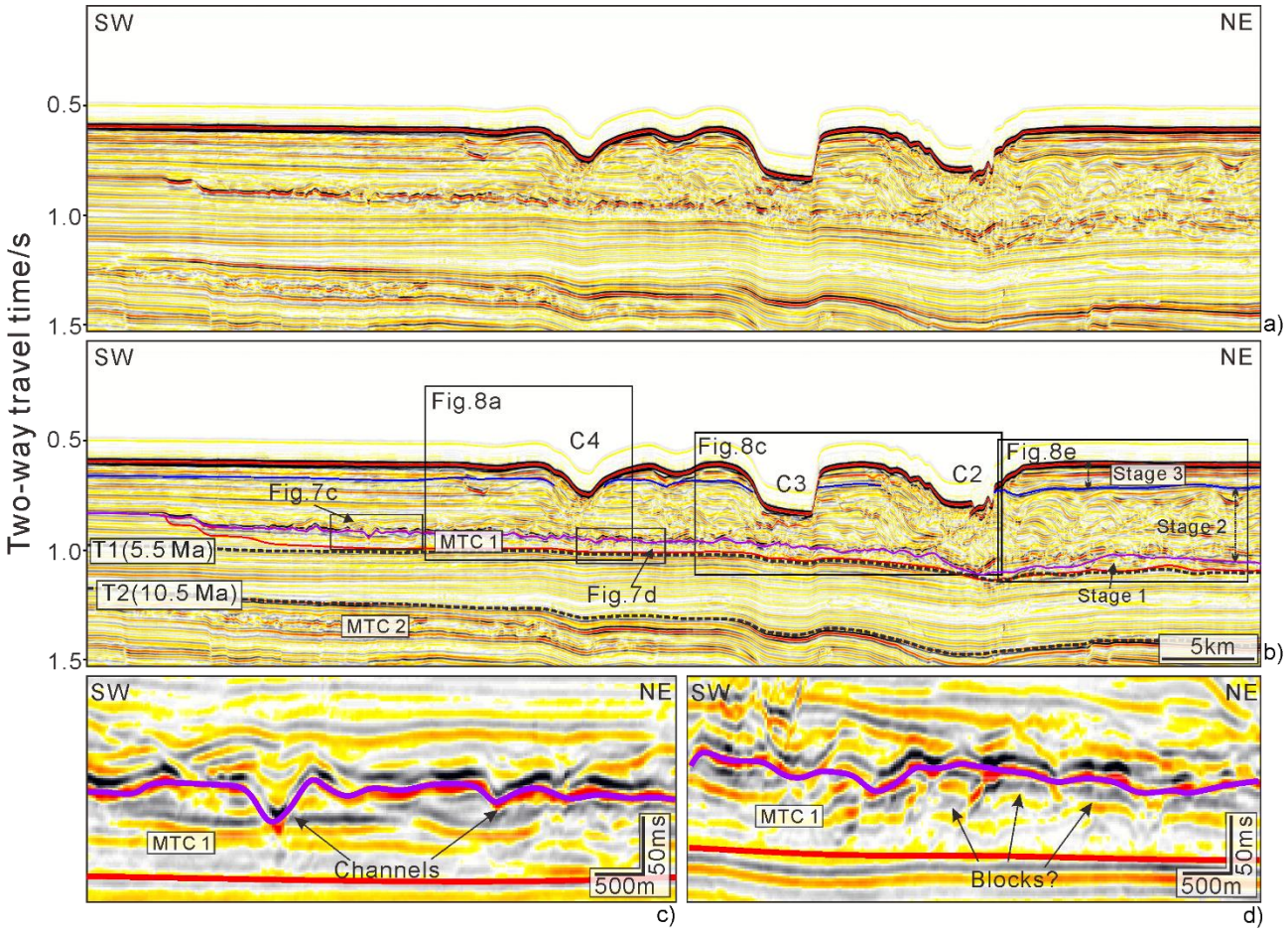

Figure 7 (a) Uninterpreted seismic profiles across C2, C3 and C4. (b) Seismic profiles highlighting two regional stratigraphic markers (5.5 Ma and 10.5 Ma) and the internal architecture in and around the submarine canyons. The purple and red solid lines mark the top and basal surface of MTC 1. (c) and (d) Zoomed-in seismic profiles showing small-scale erosive channels and putative slide blocks.

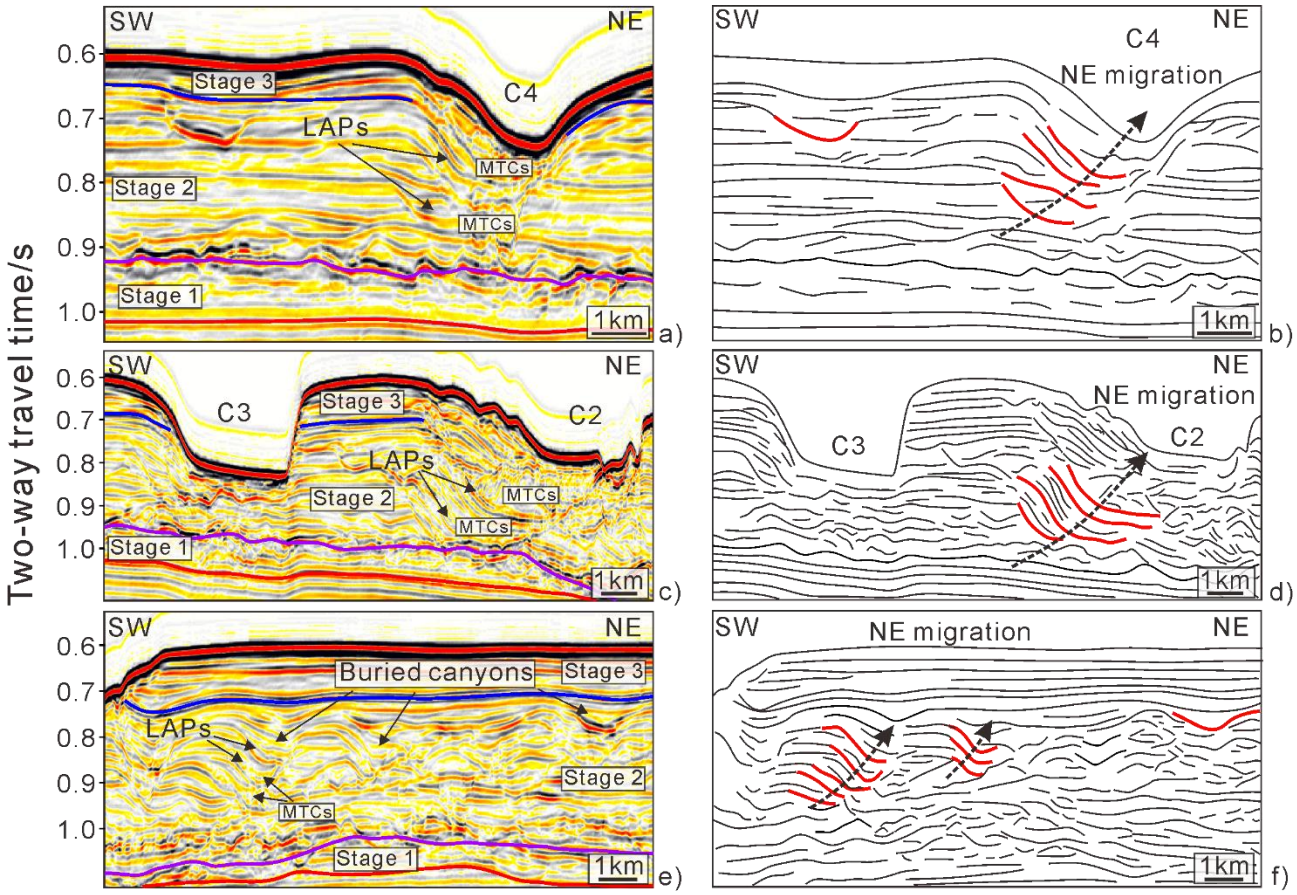

Figure 8 (a), (c) and (e) Zoomed-in seismic profiles showing the internal architecture of canyons C2, C3 and C4, plus several other buried canyons. (b), (d) and (f) Sketched interpretations of buried submarine canyons. Red solid lines mark the erosional base of migrating submarine canyons.

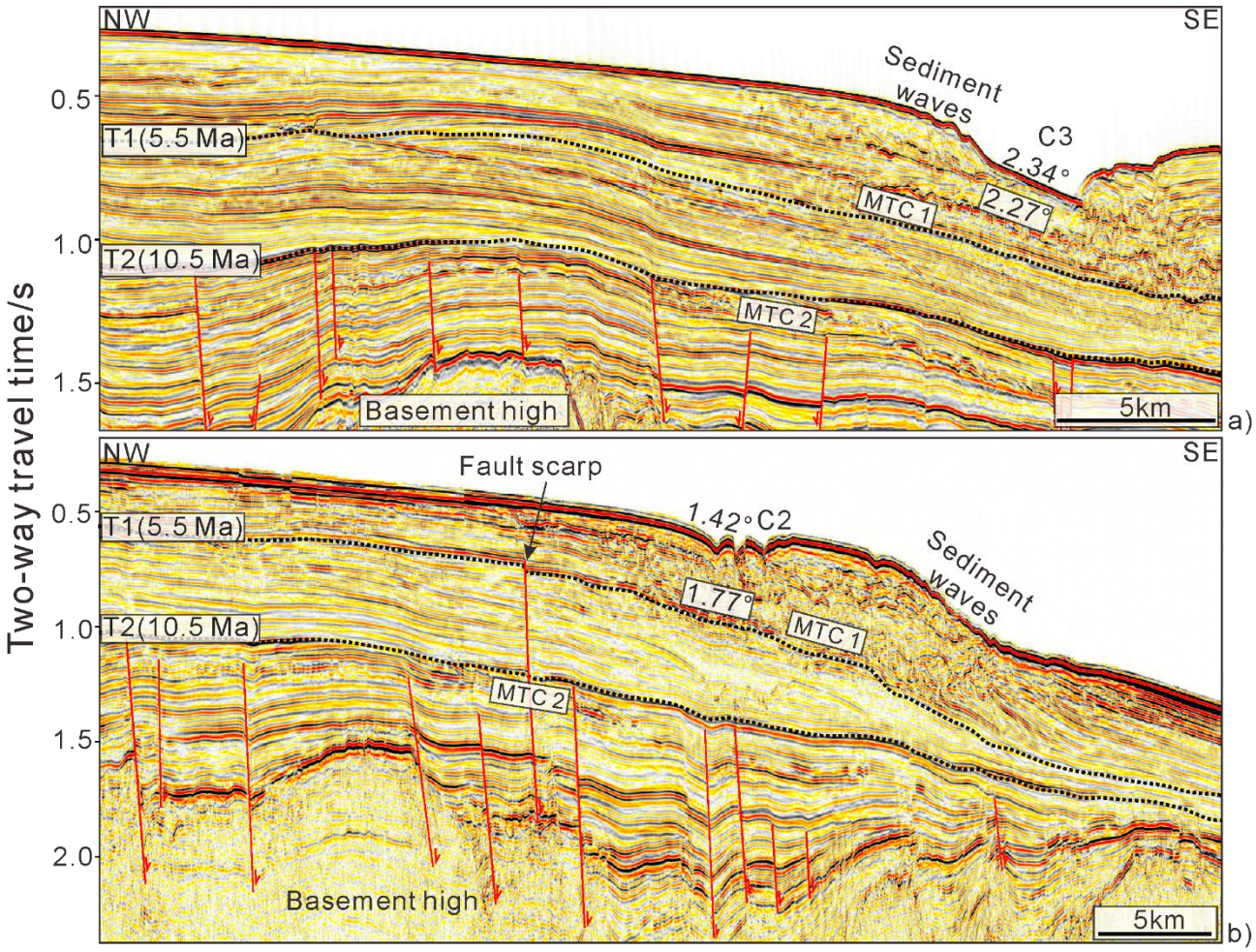

Figure 9 (a) Interpreted 2D multi-channel seismic profiles highlighting two stratigraphic markers near canyon C3 (5.5 Ma and 10.5 Ma), the presence of sediment waves and the location of MTC 1 and MTC 2. (b) Interpreted 2D multi-channel seismic profiles across canyon C2 showing sediment waves, MTC1 and MTC 2. Red solid lines on both seismic profiles mark the presence of normal faults at depth.

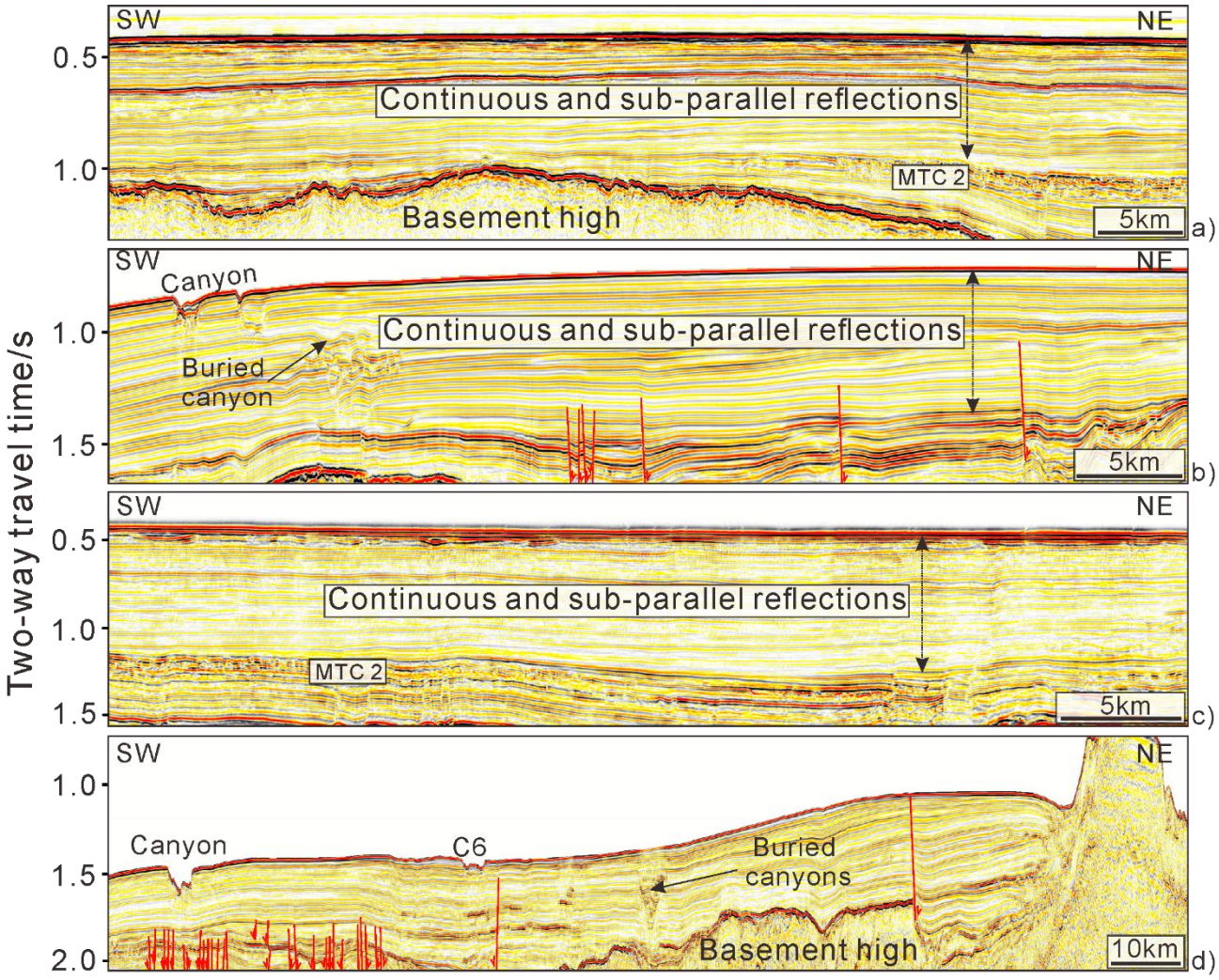

651

652 Figure 10 (a)-(c) Interpreted seismic profiles to the north, northwest and east of the isolated

653 submarine canyon system stressing the presence and relative depth of MTC 2. The strata above

654 MTC 2 are continuous and parallel. (d) Interpreted seismic profile in the southern part of the

655 canyon system showing the lower reach of C6 and a buried canyon to its northeast.

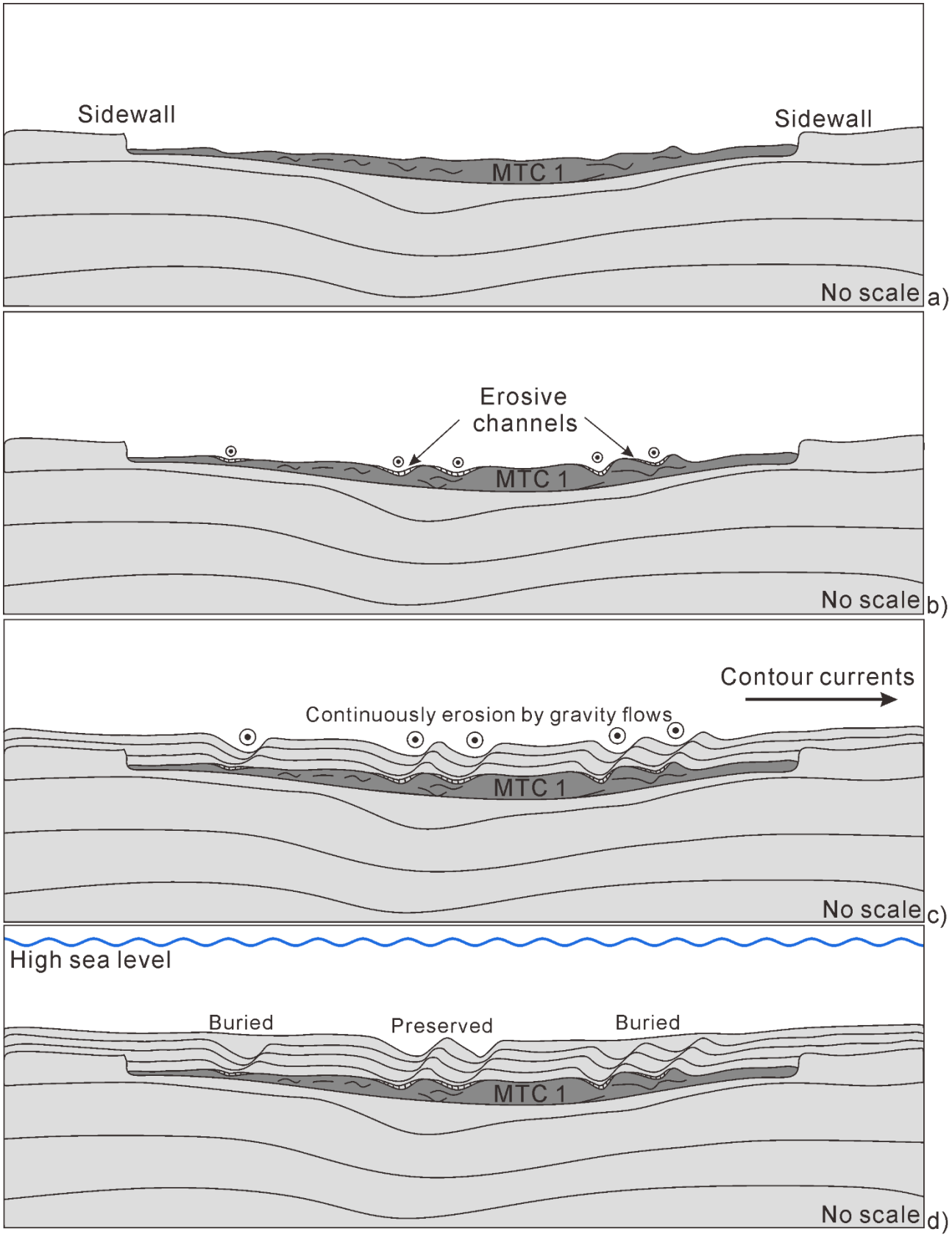

Figure 11 Schematic representation of how isolated submarine canyons evolved in the study are, northwest South China Sea. (a) A submarine landslide occurred on the continental slope

and resulted in the deposition of MTC 1. (b) Gravity flows were captured by the slide scar and led to the formation of erosive channels at the top surface of MTC 1. (c) Pre-existing erosive channels are widened and deepened and the early forms of submarine canyons are formed under continuous erosion by gravity flows. (d) Several canyons are buried, while others are preserved on the continental slope.